# Exploratory DSC investigation on the solvolytic depolymerization of PET in varied solvent systems and in the presence of model additives and contaminants

Jaime-Azuara, Antonio; Longo, Edoardo; Boselli, Emanuele; Baratieri, Marco; Pedersen, Thomas Helmer

*Published in:*
Polymer Degradation and Stability

*DOI (link to publication from Publisher):*
10.1016/j.polymdegradstab.2024.110751



*Publication date:*
2024

*Document Version*
Publisher's PDF, also known as Version of record

Polymer Degradation and Stability 224 (2024) 110751

Contents lists available at ScienceDirect

Polymer Degradation and Stability

journal homepage: www.journals.elsevier.com/polymer-degradation-and-stability

# Exploratory DSC investigation on the solvolytic depolymerization of PET in varied solvent systems and in the presence of model additives and contaminants

Antonio Jaime-Azuara [a,*], Edoardo Longo [b], Emanuele Boselli [b], Marco Baratieri [c], Thomas Helmer Pedersen [a]

[a] Department of Energy, Aalborg University, Denmark
[b] Faculty of Agricultural, Environmental and Food Sciences, Free University of Bozen-Bolzano, Italy
[c] Faculty of Engineering, Free University of Bozen-Bolzano, Italy

ARTICLE INFO

*Keywords:*
PET
High-pressure DSC
Solvolytic depolymerization
Neutral hydrolysis
Contaminants
Additives

ABSTRACT

Solvolytic depolymerization of polyethylene terephthalate (PET) is a thermo-chemical recycling route that valorizes plastic waste by recovering monomers and chemicals that can be reused for the synthesis of new polymers. This study focuses on neutral hydrolysis due to the potential environmental and economic benefits of water as depolymerization agent compared to alternative organic solvents. High-pressure crucibles were used as batch reactors in differential scanning calorimetry (DSC) to perform real-time monitoring of the thermodynamic phenomena taking place during solvolytic depolymerization of PET in varied solvent systems. PET melting point depression was found to be the main identified phenomena, with PET melting point exhibiting a drop of almost 30 °C in water and 50 °C in monoalcohol solvents like methanol and ethanol. Moreover, PET only underwent significant depolymerization prior to melting in NaOH containing systems. Gas Chromatography and Mass Spectrometry were used to study the fate of model additives and contaminants under solvolytic conditions. The uncertainty concerning these foreign substances poses a challenge for the development of PET solvolytic technologies, and the methods here provided proved to be a fast-screening technique to quantify the conversion and identify potential degradation products of model additives like 2-(2-hydroxy-5-methylphenyl) benzotriazole UV-stabilizer, 1-(methylamino) anthraquinone dye, and model contaminant (*R*)-(+)-limonene under hydrothermal conditions.

## 1. Introduction

Since the invention of the world's first synthetic plastic in 1907, the plastic industry has experienced an unapparelled growth, with continuous development of new polymer chemistries and composite materials [1]. The outstanding properties of synthetic polymeric materials, combined with their tunability to achieve specific attributes, have made them best suited for a wide variety of applications in all sectors of the economy, bringing benefits in areas such as packaging, health care, automotive, building and construction, electronics, apparel and textiles, agriculture, electricity, energy, and aerospace [2]. More than 90 % of the plastics produced worldwide are fossil-based, while 8 % come from post-consumer recycled plastics, and less than 2 % are bio-based materials [3]. Pressing environmental issues concerning climate change, resource scarcity, and degradation of natural ecosystems, are promoting the development of a more circular and efficient plastics economy that reduces fossil resources and the overall environmental impact of the plastics industry [4]. In this new paradigm, plastic consumption should be minimized, and post-consumer plastic waste becomes a valuable resource from which raw materials can be recovered to produce new plastic products.

Business-as-usual mechanical recycling technologies can recover only a limited fraction of the polymers present in post-consumer plastic waste due to contamination, material degradation, and product complexity, where films, multilayer products, colorants, and additives can be found [5]. Waste heterogeneity leads to polymer incompatibility at the time of re-extrusion and downcycling plastic materials, as product properties cannot be tailored for demanding applications. This leaves

* Corresponding author.
*E-mail address:* aja@energy.aau.dk (A. Jaime-Azuara).

https://doi.org/10.1016/j.polymdegradstab.2024.110751
Received 18 January 2024; Received in revised form 14 March 2024; Accepted 25 March 2024
Available online 27 March 2024

vast amounts of untapped plastic resources in post-consumer waste. Chemical recycling technologies use thermal, chemical, or thermo-chemical processes to significantly change the chemical structure of polymers, primarily by breaking down the chains in such a way that valuable raw materials can be recovered and purified before they are used as starting chemicals for new polymers [6,7]. The ability of chemical recycling technologies to handle relatively complex post-consumer plastic waste and to provide purified raw materials unlocks significant amounts of post-consumer plastic waste that is not currently recycled.

Solvent-based depolymerization is a chemical recycling pathway that uses a solvent to selectively break down functional groups found in the backbone structure of condensation polymers, depolymerizing them down to the original monomers [8]. Polyethylene terephthalate (PET), used primarily in food packaging and textiles, is the main source of plastic waste among condensation polymers. This is due to the short lifespan of plastic packaging and the substantial presence of PET in the textile industry, which in fact accounts for 54 % of all textile fibers and 84 % of synthetic fibers [7,9]. As a result, PET in packaging and textiles accounts for nearly 20 % of all polymer demand worldwide [3,9]. Finding a sustainable recycling solution for PET becomes paramount to accomplish a more circular plastic economy.

State-of-the-art solvolytic technologies use alcohols or water as depolymerizing agents, each of which has advantages and disadvantages in terms of product yields, energy intensity, waste generation, catalyst requirements, and environmental impact. Methods based on alcoholysis use ethylene glycol or methanol as solvents, while water-based reactions use mainly neutral or alkaline conditions. Numerous experimental investigations have been undertaken to understand the chemistry of solvolysis and the effects of different process parameters, e.g. temperature, residence time, or solvent-to-PET loading ratio, on the performance of the technology [10]. Experimental studies on PET solvolysis have been conducted mainly in a batch fashion, with the PET-solvent system loaded in the reactor, heated to the reaction temperature, held for the required retention time, and cooled. During the heating process and reaction, numerous phenomena occur that depend on the heating behavior of the mixture, such as polymer melting in the presence of solvent, polymer bond breaking, solubilization of reaction products, and potential precipitation of these products upon cooling [11]. Current batch methods do not allow for real-time monitoring of the phenomena occurring in the reactor due to the inherent pressure of solvolysis processes and only allow for analysis of yields and product composition as the reactor is treated as a black box during the experiment. New experimental methods that allow real-time monitoring of PET solvolysis could shed light on the thermodynamic processes and PET-solvent interactions mentioned above. Differential scanning calorimetry (DSC) is an analytical technique widely used in the chemical industry to measure the heat absorbed or released from the thermally activated processes that occur in the sample when it is exposed to a specific temperature program [12]. When this technique is coupled with high-pressure crucibles, it allows for the study of thermodynamic phenomena that occur during chemical reaction processes above atmospheric pressure [13,14]. The fast reaction kinetics of neutral hydrolysis of molten PET in saturated, hot liquid water offers a depolymerization solution that requires no organic solvents or catalysts and provides high monomer yields, potentially achieving lower cost and environmental impact than other solvent-based solutions [15,16].

In our previous work, chemical recycling of PET by neutral hydrolysis has shown environmental and product yield performance that is on par with the best state-of-the-art solvolysis technologies [16].

In this study, the thermodynamic phenomena of neutral hydrolysis of PET are analyzed and compared with other state-of-the-art solvent-based technologies using a high-pressure crucible in DSC. This analytical method makes it possible to estimate the onset temperature of the different thermal phenomena that occur during PET depolymerization and the extent of endothermicity/exothermicity of these processes. This paper also presents the potential use of DSC as a tool to track the fate of model PET additives and contaminants in neutral hydrolysis by integrating calorimetry results with gas chromatography of additives and contaminants and MS identification of degradation products. Finally, it will be discussed how the results and methods presented in this study could be used to develop new solvent-based processes for PET recycling.

## 2. Material and methods

### 2.1. PET preparation and characterization

Colorless Lighter C93 PET granules from Equipolymers were pulverized in a Pulverisette 14 (Fritsch) to obtain PET powder. Reducing the size of PET allows the amount of polymer added in DSC experiments to be adjusted by ±0.1 mg. PET granulates were immersed in liquid nitrogen before pulverization to increase brittleness and avoid melting due to heat generation during pulverization. Small amounts of cold granules were then loaded in the Pulverisette at a rotor speed of 8000 rpm and a metal sieve of 0.75 mm.

DSC analysis of 1) raw, 2) liquid nitrogen-treated and 3) pulverized PET samples was conducted in a Q2000 DSC (TA Instruments) to understand the impact of the downsizing process on the thermal history and polymer properties. Samples were weighed, sealed in aluminum Tzero® crucibles, and loaded into the DSC furnace along with a reference empty crucible. After temperature equilibration and a 5-min isotherm at 40 °C, the PET samples were subjected to two consecutive heating-cooling scans. A heating-cooling scan consisted of a heating scan of 10 °C/min to 280 °C followed by an active cooling scan of 20 °C/min to 40 °C. During the analysis, the furnace was subjected to a sample purge flow of $N_2$ of 50 mL/min.

### 2.2. DSC experiments

A Maia 200 F3 heat-flux DSC (NETZSCH GmbH) was used together with high-pressure 100 μL gold-plated Ni-steel crucibles rated to 100 bar. Temperature and enthalpy calibration was performed for a heating ramp of 5 °C/min using the high-pressure standard calibration kit supplied by NETZSCH. Calibration points were obtained from the thermal effect related to the fusion of standard-grade indium, bismuth, tin, and caesium chloride in the temperature range between 156 and 476 °C [17].

The PET-solvent systems presented in Table 1 were chosen for this study based on the state-of-the-art in PET solvolysis technologies [10]. Pulverized PET obtained by the methods outlined in Section 2.1 was used for the PET depolymerization experiments in the DSC. The crucible and reactants (PET, contaminants, and solvent) were weighed, controlling the filling ratio so as to obtain a saturated liquid-vapor mixture during isochoric experimental conditions. The recommended torque of 3.5 Nm was then applied to close the crucible lid using single-use seals. The crucible containing the sample was then placed in the DSC furnace together with an empty reference crucible of the same material. The weight of the crucible was measured after the experiments, and if the pre/post run mass difference was more than 2 %, the experiment was discarded because of potential leakage during the analysis. Purge and

**Table 1**
Solvent composition for the different depolymerization experiments.

| Solvent system | Solvent 1 | wt. % | Solvent 2 | wt. % | NaOH wt. % |
|---|---|---|---|---|---|
| Water [16] | Water | 100 | – | | – |
| Water-NaOH [18] | Water | 90 | – | | 10 |
| Ethanol-water-NaOH [19] | Ethanol | 51.5 | Water | 43.5 | 5 |
| Ethylene glycol [20] | Ethylene glycol | 100 | – | | – |
| Methanol [21] | Methanol | 100 | – | | – |

protective $N_2$ flows were set at 250 mL/min for all experiments. The high-pressure DSC crucibles containing the reagent mixture were subjected to an initial temperature stabilization at 50 °C for 30 min, followed by a heating scan of 5 °C/min to 310 °C, and a cooling scan without active cooling.

In addition to the PET solvolysis experiments, the hydrothermal degradation of model PET additives and contaminants in DSC was studied to illustrate the methods presented in this study. The hydrothermal degradation of the compounds shown in Table 2 and the depolymerization of PET in the presence of these additives and contaminants were studied using the same DSC methods presented previously. In the case of contaminant degradation, several experiments were conducted at different final heating temperatures, i.e. 200, 250, 300 and 350 °C, to progressively decompose the contaminants and thus facilitate the understanding of the chemical pathways under these conditions. Contaminant conversion was quantified by HPLC-MS for 2-(2-hydroxy-5-methylphenyl) benzotriazole (BT) and 1-(methylamino) anthraquinone (AQ), and GC–MS for (*R*)-(+)-limonene (LM).

### 2.3. HPLC-PDA-MS quantitation of AQ and BT and HPLC-MS/MS identification of degradation products

After DSC experiments, crucibles containing the degraded products of model contaminants were immersed in 5 mL of DMSO and shaken. The dissolved sample was then filtered and 1 mL was prepared in an LC vial for further analysis.

HPLC-PDA-MS was used to analyze the degradation products of AQ and BT. The 6465 UHPLC-QqQ/MS system (Agilent Technologies, Cernusco s/N, Italy) consisted of a 1260 Infinity II quaternary pump and a WR PDA detector, in series with a AJS (ESI)- QqQ-MS mass analyzer. Separation was performed on an Agilent Poroshell 120, SB-C18 2.1 mm × 100 mm × 2.7 μm column maintained at 30 °C. The flow rate was 0.35 mL $min^{-1}$. The mobile phase consisted of phase A (100 % ultrapure water with 0.1 % v/v formic acid), and phase B (MS-grade acetonitrile with 0.1 % v/v formic acid). The injection volume was 5 μL. The gradient program was: 0–1 min 10 %B, 1–60 min from 1 to 99 %B, 60–65 min 99 %B, 65–67 min 99 to 10 %B, 67–72 min 10 %B. Photodiode array detection was set with a spectral range of 210–700 nm, a step size of 1 nm, a slide width of 4 nm, a response time of 4 s, and prerun autobalance. The conversion of AQ and BT under hydrothermal conditions was quantified by performing calibration of the PDA response with AQ and BT standards. The calibration methods and results are given in the supplementary material.

Identification of potential degradation products was performed using tandem MS. For the positive ionization mode in the mass spectrometer, the ESI ionization potential was set at +3500 V and VCharging at 1000 V. The in-source gas temperature was 340 °C, the gas flow was 13 L $min^{-1}$, the nebulizer was set at 50 psi, the sheath gas temperature was 350 °C, and sheath gas flow was 12 L $min^{-1}$. For the negative ionization mode, the ESI ionization potential was set at −2500 V and VCharging at 0 V. The in-source gas temperature was 260 °C, gas flow 4 L $min^{-1}$, nebulizer was set at 35 psi, sheath gas temperature was 300 °C, and sheath gas flow was 12 L $min^{-1}$. The analyses were run in full scan mode with a mass range of *m/z* 50–750, a scan time of 500 ms, a fragmentor potential of 135 V, and a cell acceleration voltage of 5 V. The analyzer was calibrated daily with the calibration mixture provided by the vendor. MS/MS analysis was run by applying unit resolution to the first quadrupole, and *m/z* 50 – [precursor mass + 5 Da] as the scan range for the second quadrupole. The applied collision energy was always 30 eV. Along with the MS/MS analysis, the PDA trace was used to identify the main compounds formed during the degradation of the products, using their UV–vis spectra.

**Table 2**
Model PET additives and contaminants considered in the current study.

| Contaminant family | Chemical compound | Abbreviation | CAS number |
|---|---|---|---|
| Use application [22] | (*R*)-(+)-Limonene | LM | 5989-27-5 |
| Benzotriazole UV-stabilizer [23] | 2-(2-hydroxy-5-methylphenyl) benzotriazole | BT | 2440-22-4 |
| Anthraquinone Dye [24] | Disperse Red 9, or 1-(methylamino) anthraquinone | AQ | 82-38-2 |

### 2.4. GC–MS

After the DSC experiments, the crucibles containing the degraded products of LM were immersed in 5 mL of dichloromethane (DCM) and shaken to dissolve the sample. Since DCM and water are immiscible, the dissolved sample was collected while avoiding water, filtered, and 1 mL was prepared in a GC vial for further analysis.

A 7890A GC coupled to a 5975 MS, both from Agilent (Wilmington, DE, USA) was used for GC–MS analysis. Volatile compounds were analyzed by separation on a MEGA-WAX Spirit capillary polar column (0.30 μm/0.18 mm/40 m; MEGA S.r.L., 20025 Legnano, Milano, Italy). The carrier gas (helium) was set at a constant flow rate of 0.7 mL/min. The injector was set in split mode (10:1). The injection volume was 1 μL. The inlet temperature was 240 °C. The temperature program for the GC oven was as follows: 40 °C for 0.2 min, then increased to 220 °C at a rate of 1.5 °C/min and finally up to 240 °C at 15 °C /min. The electron ionization was 70 eV and the ion source temperature was set at 230 °C. The detector mass range was 34–360 *m/z*; the quadrupole temperature was 150 °C, and the acquisition rate was 1 scan/s. Compounds were identified by injection of standard (limonene) or comparison of spectral and retention indices with the NIST database (e.g. *p*-cymene). The saturated alkanes series (C8-C40, in DCM) was used to calculate retention indices. The conversion of LM under hydrothermal conditions was quantified by performing MS response calibration of the LM base ion fragment *m/z* 68 with the LM standard. The calibration method and results are given in the supplementary material.

## 3. Results and discussion

### 3.1. Characterization of pulverized PET

The DSC traces of raw PET, liquid nitrogen treated PET and pulverized PET are presented in Fig. 1. During the first heating scan at 10 °C/min, no $T_g$ or hot crystallization were observed for any of the samples, demonstrating the high crystallinity of the starting material. All the samples showed a double melting peak, which could be attributed to the presence of different crystal structures caused by the specific PET production process and the thermal history of the material [25,26]. After production, PET granules gradually cooled down and crystallized from the outside to the inside. Due to the poor heat transfer of polymeric materials, the core of the granules would have much more time to crystallize than the periphery, leaving the latter in a “stressed” position that could lead to poor crystal structures. The first melting peak of the pulverized sample at 235 °C was considerably less pronounced than the other PET samples, while the second peak at 250 °C was approximately the same for all. In addition, the pulverized PET sample was the only one to show a hot-crystallization peak during the cooling scan. On the one hand, the enthalpy difference of the first melting peak between the pulverized sample and the other PET samples could be triggered by the reduction of internal stresses and the local heat generated during the pulverization process. On the other hand, the exothermic crystallization peak during the cooling scan suggests a higher mobility of polymer chains that facilitates melt crystallization in the pulverized sample compared with the non-pulverized samples. The increased mobility is likely due to mechano-chemical fragmentation of the polymer chains during the pulverization process, which would also lead to a reduction in

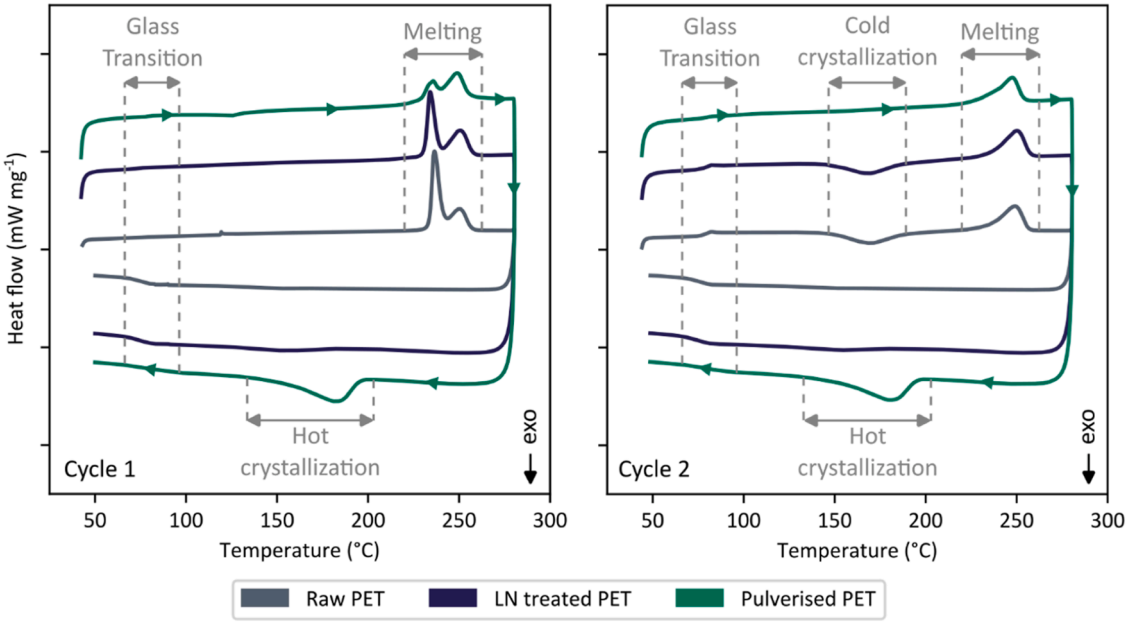


**Fig. 1.** DSC traces of raw PET granulates, PET granulates after liquid nitrogen treatment, and pulverized PET. Results are shown for the first (left) and second (right) heating-cooling scan cycles. The arrows on the DSC trace indicate the direction of the heating-cooling scans.

the average molecular weight [27]. The degree of degradation is unknown, however, as even a small amount of initial crystallization sites could have a huge impact. Finally, raw and liquid nitrogen-treated PET showed the same amount of crystallinity and the same crystallization temperature in the second heating scan, thus the same thermodynamic behavior.

### 3.2. PET depolymerization in subcritical water

Terephthalic acid (TPA) and ethylene glycol (EG) are the most widely used starting building blocks for PET synthesis. In addition to TPA and EG, other starting materials such as dimethyl terephthalate (DMT) and bis(2-hydroxyethyl) terephthalate (BHET) can also be used for PET synthesis using different synthesis routes [28]. Under solvolytic depolymerization conditions, PET is broken into its original constituents, but the final product depends on the method used. Under neutral

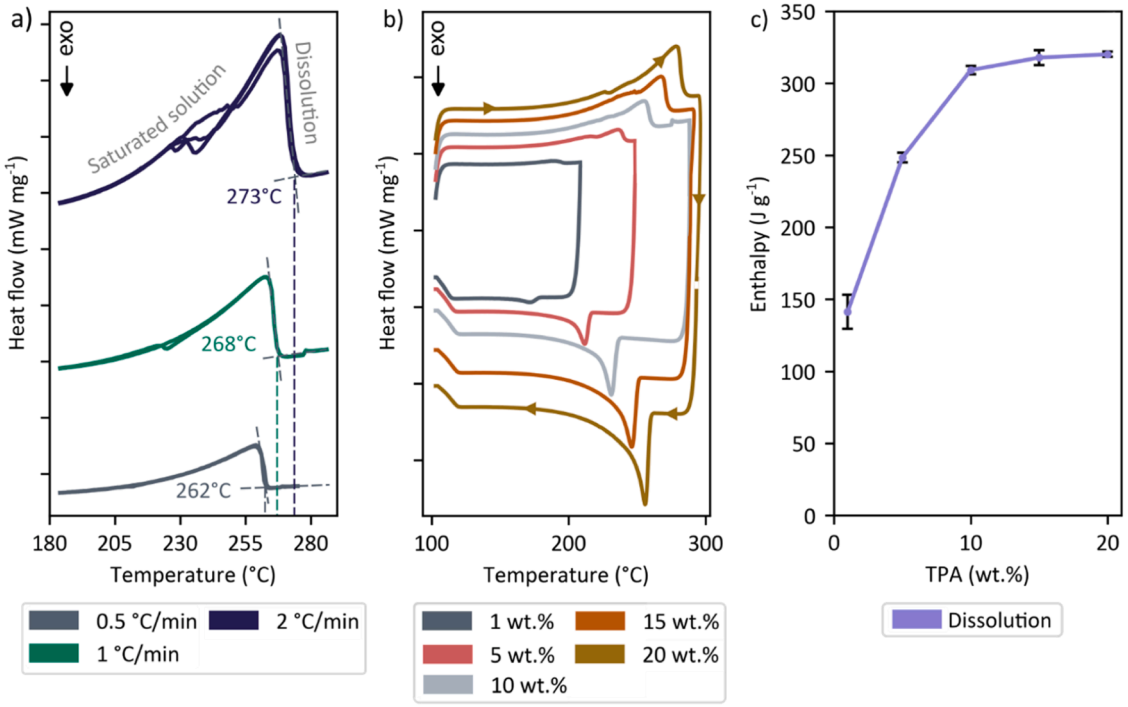


**Fig. 2.** Results of TPA solubility experiments in water. a) DSC traces of TPA 15 wt.% with heating ramps of 0.5, 1, and 2 °C/min.
b) TPA solubility with a heating ramp of 2 °C/min at different TPA concentrations 1, 5, 10, 15, and 20 wt.%. The arrows on the DSC trace indicate the direction of the heating-cooling scans. c) Dissolution enthalpy of TPA for different TPA concentrations in water.

hydrolysis conditions, TPA and EG are the main depolymerization products, but under alkaline conditions, TPA reacts with the base to form terephthalate salt as main product. For alcohol-based depolymerization technologies, the diester of TPA and alcohol solvent is formed as the main product, while DMT and BHET are the main products of methanolysis and glycolysis, respectively. All these depolymerization products exhibit some solubility in the depolymerization solvent, which triggers heat exchange upon heating and cooling, with endothermic enthalpy of solubilization and exothermic enthalpy of precipitation, respectively.

Since dissolution of TPA in water is a crucial phenomenon during neutral hydrolysis of PET, DSC analyses of different concentrations of TPA in water were performed at various heating ramps. To maintain solution at its saturation point during heating and thus determine the saturation temperature for a given concentration would require an infinitely slow heating rate. Therefore, the finite heating rate of a DSC instrument allows only for nonequilibrium measurements, obtaining saturation temperature values slightly higher than the actual saturation temperature of the solution. The difference between the calculated and real value of the saturation temperature vanishes the slower the heating ramp and in cases where the dissolution kinetics are fast.

Fig. 2(a) shows the DSC traces of an aqueous solution with 15 wt.% TPA in which the saturation temperature is calculated from the DSC curves following the method reported by Mohan et al. [29]. This figure shows that reducing the heating ramp results in lower values of saturation temperature and the fact that TPA dissolution kinetics is slower than the heating ramp. Moreover, the fluctuations observed in the DSC trace when the heating ramp is 2 °C/min, and to a lesser extent when the ramp is 1 °C/min, suggest the presence of a non-homogeneous crystal distribution, since a flat, regular line would be obtained if the heating ramp followed the dissolution kinetics and all crystals had the same size. The saturation temperature for a solution containing 15 wt.% TPA is predicted to be 260.5 °C based on the work of Takebayashi et al. [30]. This temperature is in good agreement with the saturation temperature of 262 °C obtained in this study from the experiment with 15 wt.% TPA and heating ramp 0.5 °C/min. By increasing the heating ramp to 2 °C/min, the difference becomes more prominent, and the predicted saturation temperature of 260.5 °C is 12.5 °C lower than the temperature measured in the experiment, as shown in Fig. 2(a). These results highlight the need to perform slow heating ramps to obtain accurate solubility results, which in return weakens the DSC signals and makes the analysis time-consuming. Since the objective of this study was not to perform a detailed investigation of the solubility of TPA in subcritical water, but to better understand the different phenomena that occur during PET depolymerization, DSC was used only to estimate the endothermicity of TPA dissolution in water, which was not affected by the heating rate of the experiment. This approach allowed representative results of the enthalpy of dissolution to be obtained in a reasonable time by using faster heating ramps.

Fig. 2(b) shows the heating and cooling scans for different TPA concentrations after a heating ramp of 2 °C/min, showing both TPA solubilization endotherms and precipitation exotherms. Fig. 2(c) summarizes the results of the dissolution enthalpy for different concentrations of TPA. The significant difference in dissolution enthalpy between the experiments with 1 and 5 wt.% TPA and those at higher concentration of TPA could be due to: 1) the limited solubility of TPA at low temperatures leads to weak thermal effects of TPA dissolution that are damped by the heat capacity of water, 2) the enthalpy of dissolution, which could increase with temperature as described by Kirchhoff's law [31]. For the experiments with 10, 15 and 20 wt.% TPA, the enthalpy of dissolution is similar and is around 315 J/g TPA. Considering this result as a representative enthalpy value of the dissolution process, if PET were completely depolymerized under neutral hydrolysis conditions, there would be an endothermic TPA dissolution process of 274 ± 5 J/g PET.

During the heating scan, several thermodynamic phenomena associated with the polymer and PET-water interaction were expected: 1) thermal history of PET, 2) melting of PET, 3) depolymerization reaction of PET, and 4) solubilization of reaction products. All these processes involve heat exchange and, therefore, can be detected by DSC analysis. The first phenomenon observed upon heating is the melting of PET, which is an endothermic process. Melting of the polymer results in an endothermic double peak, which can be observed in the DSC trace of Fig. 3. The origin of the double melting peak was discussed in Section 3.1, and from the DSC analysis of the PET material in Fig. 1 the onset temperature of the melting process was 230 °C. However, from the results shown in Fig. 3, the melt initiation of PET was reduced to 200 °C in the presence of water.

This behavior can be explained by the Flory-Huggins melting point depression theory, according to which the swelling of the polymer allows solvent molecules to penetrate inside the polymer bulk and, due to the mixing and interaction between polymer and solvent molecules, the melting point of PET is reduced [32]. At equilibrium, the chemical potentials of the polymer repeating unit in both phases, liquid and crystalline, are equal. This condition fulfills at temperature $T_m$. For pure polymer $T_m = T_m^0$, which is the standard melting point of the polymer. If the composition of the liquid phase varies due to the presence of a solvent, the chemical potential of the liquid phase will be lower than that of the pure polymer and therefore $T_m$ will decrease to reestablish the equilibrium condition between the crystalline and liquid phase [33,34]. The adequacy of DSC to experimentally quantify the melting point depression of PET in the presence of a solvent could be exploited to design custom reagent feed systems, and tune process temperatures to take advantage of this phenomenon.

In addition to the melting endotherm, another endothermic peak was observed at higher temperatures. In the molten state, hydrolysis of ester bonds should occur at a sufficiently high rate to be observed in the DSC trace. In addition, TPA, generated by PET depolymerization, will lead to an endothermic dissolution process, as previously described. For six independent repetitions of the PET depolymerization reaction under hydrolytic conditions, the endothermic energy after PET melting was FFated to be 91 ± 11 J/g PET based on the integration of DSC peaks, which is significantly lower than the endotherm expected from TPA dissolution alone (274 ± 5 J/g PET). Thus, there is a simultaneous exothermic process that counteracts some of the energy required for TPA dissolution. Numerous kinetic studies on the hydrolysis of molten PET have reported that the equilibrium constant of the depolymerization reaction decreases with temperature, indicating that the hydrolytic depolymerization of molten PET is an exothermic process [35–38]. These results support the hypothesis that the exothermic nature of the reaction provides some of the energy required for the endothermic dissolution of TPA. Kao et al. reported that the heat release during hydrolysis of PET ester bonds was 599 J/g PET, whereas the results presented here suggest that this energy is about 183 J/g PET [37].

Three preliminary tests of PET depolymerization in water were conducted to evaluate the conditions that provided the best trade-off between signal intensity, baseline shape and signal delay due to thermal inertia and heat transfer limitations. Fig. 4 shows the DSC heating scan for the 10 wt.% PET-water system after different heating ramps of 2, 5, and 10 °C/min. The 5 °C/min heating ramp provided significant signal intensity, better baseline shape than the 10 °C/min ramp and showed no delay in the PET melting peak signal compared with the 2 °C/min heating ramp. Therefore, the heating ramp of 5 °C/min was chosen for solvolytic depolymerization experiments. Nevertheless, reaction and solubilization thermal effects are affected by the heating ramp since these are time dependent processes. If a step of 50 °C is considered, it would take 25, 10 and 5 min to be completed at heating rates of 2, 5 and 10 °C/min, respectively. Therefore, when the heating ramp is lower, PET is exposed to depolymerization for a longer time before the sample reaches a certain temperature. This explains why the last peak related to the reaction takes place at 250 °C for the heating ramp of 2 °C/min compared to 275 °C in the experiment with a heating ramp of 5 °C/min.

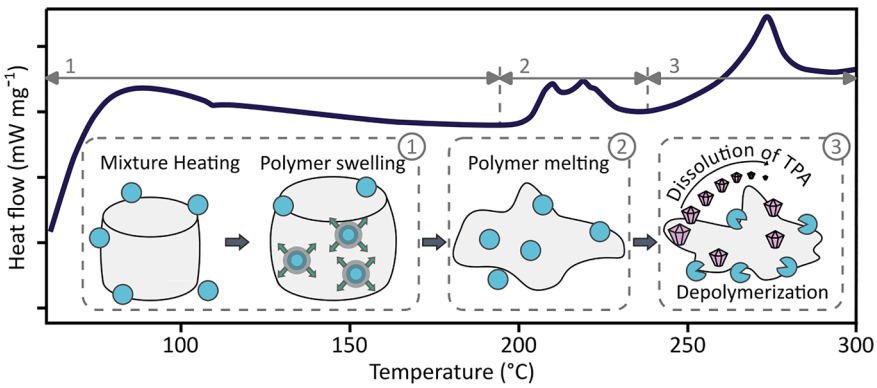


**Fig. 3.** Thermodynamic phenomena taking place during DSC experiments of PET neutral hydrolysis in subcritical water.

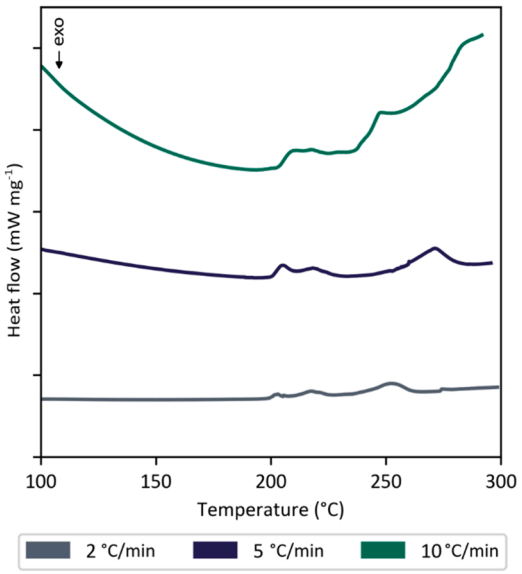


**Fig. 4.** DSC heating scan with ramps of 2, 5, and 10 °C/min for the PET-water system.

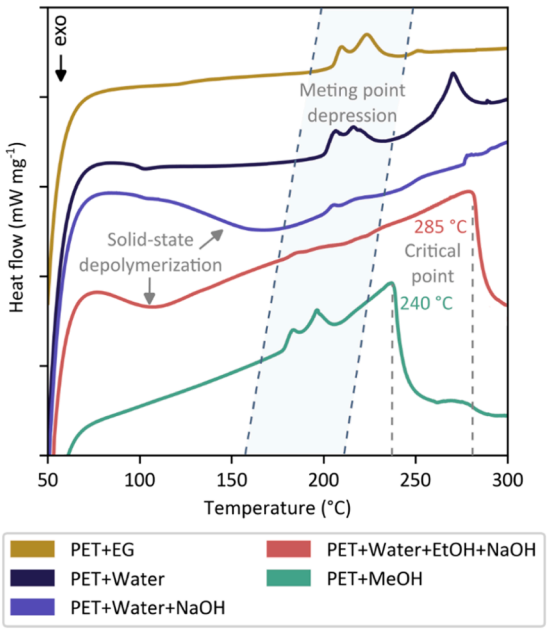


**Fig. 5.** DSC traces for the different PET-solvent systems considered in this study.

### 3.3. PET depolymerization in different PET-solvent systems

Fig. 5 shows the DSC traces of PET depolymerization in different PET-solvent systems compared to the PET-water system. In all experiments, the temperature profiles and PET weight percentage were kept constant with a heating ramp of 5 °C/min and 10 wt.% PET, respectively. Table 3 presents the onset temperature of the PET melting peak and the enthalpy associated with this process for all PET-solvent systems. Regarding melting point depression, it is worth noting that monoalcohol systems, represented here by methanol and ethanol, showed significant depression of PET melting temperature compared to water and ethylene glycol.

In the presence of a solvent, depolymerization occurs mainly on the surface of PET particles before melting, leaving the core of PET particles unreacted and thus showing an enthalpy of melting inversely proportional to PET conversion. Ügdüler et al. reported 68 % PET conversion at 80 °C and 20 min retention time using a similar solvent mixture of ethanol, water and NaOH. The DSC results in Fig. 5 and Table 3 support the above results, as the ethanol-water-NaOH experiment showed the lowest PET melting enthalpy, meaning that most of the polymer was already depolymerized before reaching the PET melting temperature. A similar but less pronounced result was obtained during the water-NaOH experiment. These results indicate that solid-state depolymerization of PET in the presence of NaOH is remarkable and is detected in the DSC as a progressive exothermic baseline deviation before PET melting for both ethanol-water-NaOH and water-NaOH solvent systems. Karayannidis et al. used alkaline hydrolysis at 200 °C for 1 h, achieving a TPA yield of 97.9 %, which confirms that significant solid-state depolymerization takes place in the presence of NaOH [18]. Aguado et al. achieved similar results at 150 °C for 2 h, with a TPA yield of 91.9 % [39]. Nevertheless, Pereira et al. just obtained 3 % TPA yield when using neutral hydrolysis at similar process condition (200 °C, 2 h). By rising the reaction temperature to 260 °C, which is beyond the melting point of PET, the TPA yield was increased to 60 % for a reaction time of 30 min [15].

**Table 3**
Melt onset temperature and meting enthalpy for different PET-solvent systems.

| Solvent system | $T^{o}_{onset}$ [°C] | $T_{onset}$ [°C] | $\Delta T_{onset}$ [°C] | $\Delta H_m$ [J/gPET] |
|---|---|---|---|---|
| PET | 228.4 | – | – | 47.5 |
| PET + water | – | 200.9 | −27.5 | 49.9 |
| PET + water + NaOH | – | 201.2 | −27.2 | 13.3 |
| PET + water + ethanol + NaOH | – | 177.8 | −50.6 | 7.4 |
| PET + ethylene glycol | – | 205.0 | −23.4 | 70.9 |
| PET + methanol | – | 178.4 | −50.0 | 49.3 |

Phase changes are endothermic or exothermic processes that can be detected by the DSC equipment. In Fig. 5, DSC traces of ethanol-water-NaOH and methanol depolymerization experiments showed a sudden decrease in heat flow at 240 °C and 285 °C, respectively. This phenomenon fits well with the predicted critical temperature for methanol at 240.2 °C, beyond which the isochoric heat capacity of methanol undergoes a drastic decrease [40]. Similar behavior was observed for the ethanol-water-NaOH mixture at 285 °C, which was 44.2 °C higher than the critical temperature of ethanol due to the presence of water [41,42].

### 3.4. DSC degradation of model PET additives and contaminants

The degradation of model PET additives and contaminants was performed in DSC following a heating ramp of 5 °C/min to 200, 250, 300 and 350 °C followed by a cooling step. The objective was to understand the degradation of these compounds under hydrothermal conditions and to evaluate whether DSC traces could be used as a tool to predict the decomposition of contaminants in solvolytic depolymerization of PET.

Fig. 6(a) shows the DSC traces of 5 wt.% 1-(methylamino) anthraquinone (AQ), 2-(2-hydroxy-5-methylphenyl) benzotriazole (BT), and (*R*)-(+)-limonene (LM) in water for the experiment at 350 °C. LM is already liquid at room temperature, but AQ and BT exhibit endothermic melting peaks upon heating to 162 °C and 132 °C in the presence of water, while the melting points of their pure forms are 170.1 °C and 125.5–133 °C, respectively [43,44]. AQ experienced melting point depression due to the presence of water while the melting point of BT remained unchanged. At high temperature, ripples appeared in the DSC traces in all cases, which could be attributed to contaminant degradation reactions. The rippling behavior started at 245–260 °C for AQ, 225–240 °C for BT, and 270–280 °C for LM. To demonstrate whether the ripples could belong to heat of degradation reactions, quantitative analysis of model contaminants was performed by HPLC-UV-MS and GC–MS analysis. The conversion of contaminants shown in Fig. 6(b) was calculated by comparing the mass of material loaded in the crucible and the amount of unreacted contaminant quantified after the experiment. BT is not presented in Fig. 6(b) since the conversion trends were not conclusive. Nevertheless, conversion was between 0 and 10 % for all the experiments, confirming the great stability of BT under hydrothermal conditions. On the other hand, AQ and LM showed degradation already at 200 °C, with LM undergoing 100 % conversion at 350 °C.

Fig. 6(c) shows the results of DSC experiments in which PET was subjected to hydrothermal depolymerization in the presence of the selected additives and contaminants. In these experiments, 1 wt.% of additives and contaminants was used, equal to 10 wt.% of the PET present in the crucible considering a PET heavily loaded with these compounds [45]. It is possible to identify the endothermic melting peaks of AQ, BT and PET, with PET undergoing enhanced melting point depression in the presence of limonene. However, the thermal effects of the different phenomena overlap, making it difficult to isolate the individual effects.

### 3.5. HPLC-MS/MS and GC–MS identification of degradation products

Identification of the main degradation products from AQ, BT and LM treatment under hydrothermal conditions was performed to support the quantification results and elucidate the potential pathways of additives and contaminants. Analysis of the degradation products of AQ and BT was performed by PDA and HPLC-MS/MS in positive ionization mode, and potential candidates were tentatively assigned based on the interpretation of the intact precursor ion and MS/MS fragment ions. The corresponding MS spectra and chromatograms are given in the supplementary material.

Table 4 reports the peaks identified in the degradation of AQ. The main degradation product of AQ, as observed from UV–vis and LC-MS traces, was *m/z* 234 at 21.8 min. This would correspond to intramolecular cyclization, involving the loss of four hydrogen atoms (e.g. as two molecular hydrogen molecules). A tentative representation of this phenomenon is shown in Fig. 7. However, further testing and analyses are needed to validate this hypothesis.

The peaks identified for BT degradation are shown in Table 5. The main product of BT degradation, observed by comparing UV–vis traces and MS relative abundances, was the *m/z* 240 (ESI+) signal at 24.7 min. As a tentative explanation, this product could be the result of the oxidation of the *p*-methyl group in the 4-methylphenol moiety to the corresponding aldehyde, as shown below [46,47]. However, further investigation would be needed to verify this hypothesis (Fig. 8).

GC–MS (EI ionization) was used to analyze the degradation products of LM and Table 6 shows the identified peaks. The degradation products

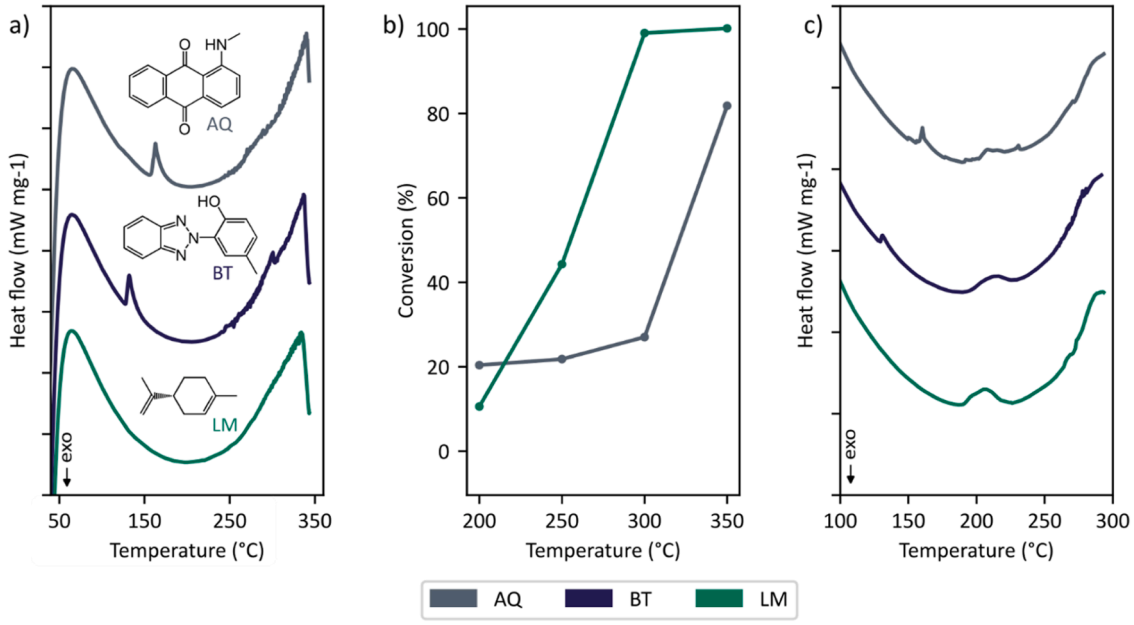


**Fig. 6.** DSC experiments of model PET additives and contaminants: a) DSC traces of hydrothermal degradation of additives and contaminants, b) Conversion at different temperatures, and c) PET hydrothermal depolymerization in the presence of additives and contaminants.

**Table 4**
HPLC-MS/MS peaks identified in the degradation of AQ, the corresponding retention time (RT) and tentative assignments.

| Assignment | Average RT (±0.1 min) | UV–vis l max (±2 nm) | Precursor ion (±0.4 *m/z*, ESI+) | Fragment ions (±0.3 *m/z*, ESI+, CE = 30 eV) |
|---|---|---|---|---|
| Loss of [2H + O] | 18.0 | 430 | 220 | 220, 193, 165 |
| Intramolecular cyclization | 21.8 | 463 | 234 | 234, 219, 193, 179, 165 |
| Intramolecular rearrangement | 24.9 | 470 | 238 | 238, 223, 195, 193, 167, 165, 134, 105 |
| Addition of an oxygen - radical | 25.5 | 503, 370 | 253 | 253, 238, 235 |
| AQ | 27.8 | 517 | 238 | 238, 223, 220, 195, 193, 167, 165 |

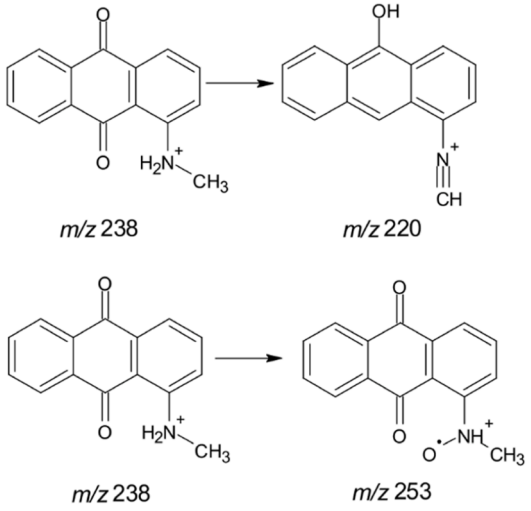


**Fig. 7.** Proposed tentative degradation products of AQ under hydrothermal conditions.

**Table 5**
HPLC-MS/MS peaks identified in the degradation of BT, the corresponding retention time (RT) and tentative assignments.

| Assignment | Average RT (±0.1 min) | UV–vis l max (±2 nm) | Precursor ion (±0.4 *m/z*, ESI+) | Fragment ions (±0.3 *m/z*, ESI+, CE = 30 eV) |
|---|---|---|---|---|
| BT | 32.0 | 336, 298 | 226 | 226, 197, 183, 154, 120, 107, 92, 79, 77, 65 |
| Aldehydic derivative | 24.7 | 327, 276 | 240 | 240, 212, 183, 166, 154, 139, 129, 93, 65 |

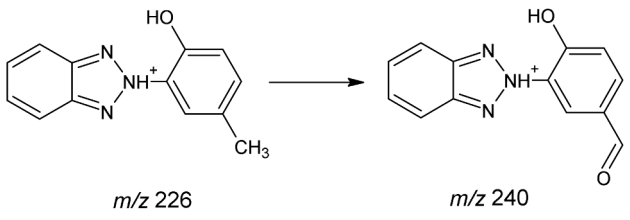


**Fig. 8.** Proposed tentative degradation products of BT under hydrothermal conditions.

**Table 6**
GC–MS peaks identified in the degradation of LM, the corresponding retention time (RT), retention index (RI) and tentative assignments.* Measured RI were calculated against the linear alkanes series (C8-C40).

| Assignment | Average RT (±0.1 min) | Average RI (±1) * | Base mass (±0.3 *m/z*, EI = 70 eV) |
|---|---|---|---|
| *p*-menth-3-ene | 10.4 | 1104 | 95 |
| *p*-menth-1-ene | 14.1 | 1200 | 95 |
| α-terpinene | 16.8 | 1265 | 121 |
| LM | 18.0 | 1292 | 68 |
| γ-terpinene | 21.4 | 1372 | 93 |
| *p*-cymene | 23.2 | 1415 | 119 |
| 2-carene | 24.5 | 1446 | 121 |

were tentatively assigned based on correspondence with the NIST database and Retention Index (RI) calculation, and their spectra are given in the supplementary material. The main degradation product of LM, as observed from the GC–MS traces, was *p*-cymene. Considering the stabilization that corresponds to the formation of the aromatic structure, *p*-cymene could be considered the end result of degradation, while the other compounds would represent intermediate stages of degradation, as shown in Fig. 9 [48,49].

## 4. Conclusions

Thermodynamic phenomena involved in the hydrothermal depolymerization of PET were successfully identified by using high-pressure crucibles and DSC methods. The experiments provided an estimate of the onset temperature and relative heat exchange for the key thermal processes: PET melting, depolymerization, and product dissolution. In addition, DSC allowed comparison of these thermodynamic phenomena for several state-of-the-art PET-solvent systems. In the presence of a solvent, melting point depression was one of the main phenomena identified. The decrease in PET melting temperature was most pronounced in the presence of monoalcohol solvents like methanol and ethanol (up to 50 °C) compared to standard PET. Moreover, PET underwent significant depolymerization before melting only in NaOH containing systems. All these results are valuable for the design of batch and continuous systems for PET solvolysis in the future, as PET melting plays a crucial role in the depolymerization kinetics, and energy estimates for the system could be obtained from DSC experiments. In future DSC studies focusing on solvolytic depolymerization of PET, monomer quantification techniques tailored for each solvolysis system would expand the thermodynamic results with accurate assessment of the

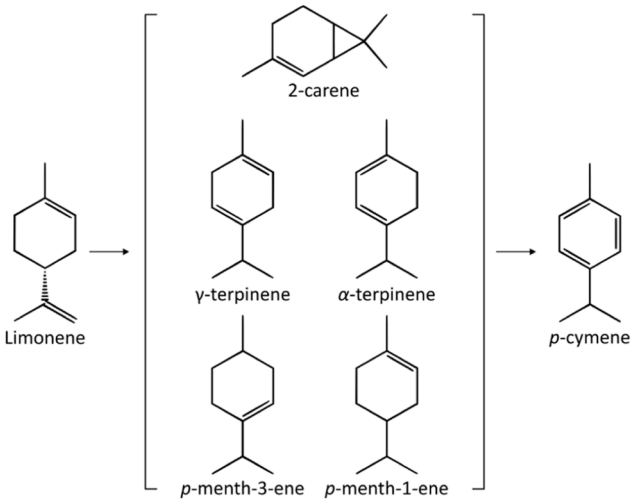


**Fig. 9.** Proposed degradation pathway of LM to *p*-cymene under hydrothermal conditions.

degree depolymerization.

The hydrothermal degradation of model PET additives and contaminants was studied with DSC. Comparing the DSC traces and conversion results of different compounds, it is concluded that DSC alone does not provide sufficient information on the degradation of additives and contaminants. This could be due to the low concentration of these contaminants, which would lead to a poor DSC response, or the high complexity of DSC traces when PET is also present, which makes it difficult to differentiate the various phenomena. This demonstrate the uncertainty when dealing with real plastic waste, where additives and contaminants are unpredictable and follow unknown degradation pathways. These results also highlight the need for industry regulation to promote harmonization of plastic design.

The degradation of PET additives and contaminants was further analyzed by MS methods. Intramolecular cyclization was identified as a potential degradation pathway of AQ, while oxidation to aldehydic derivative was probably the main degradation pathway of BT, despite its high stability. In addition, *p*-cymene was identified as an end product of LM after hydrothermal treatment. The identification of potential degradation pathways aimed to be a starting point for future investigation, and further analyses would be required to confirm and fully characterize degradation products.

In short, DSC enables the simultaneous execution of chemical reactions while monitoring and analyzing all the thermal effects taking place. By coupling DSC with chromatography and MS analytical techniques, a more holistic understanding of reaction thermodynamics, temperature onset of thermal phenomena, and product composition is achieved. Overall, DSC coupled with high-pressure crucibles has the potential to become a rapid screening tool for evaluating new solvent systems for PET depolymerization, accelerating the development of future solvent-based recycling technologies.

## CRediT authorship contribution statement

**Antonio Jaime-Azuara:** Investigation, Data curation, Conceptualization, Methodology, Project administration, Validation, Visualization, Writing – original draft, Writing – review & editing. **Edoardo Longo:** Writing – review & editing, Conceptualization, Data curation, Investigation, Methodology, Validation, Visualization, Writing – original draft. **Emanuele Boselli:** Writing – review & editing, Validation, Resources, Methodology, Conceptualization. **Marco Baratieri:** Writing – review & editing, Validation, Supervision, Resources, Methodology, Conceptualization. **Thomas Helmer Pedersen:** Supervision, Methodology, Funding acquisition, Validation, Writing – review & editing.

## Declaration of competing interest

The authors declare the following financial interests/personal relationships which may be considered as potential competing interests:

Thomas Helmer Pedersen reports financial support was provided by Innovation Fund Denmark. If there are other authors, they declare that they have no known competing financial interests or personal relationships that could have appeared to influence the work reported in this paper.

## Data availability

Data will be made available on request.

## Acknowledgments

This research was financially supported by Innovation Fund Denmark, Innomission 4 (TRACE), under the “PETfection” project [grant number: 1153-00001B].

## Supplementary materials

Supplementary material associated with this article can be found, in the online version, at doi:10.1016/j.polymdegradstab.2024.110751.

## References

[1] R. Geyer, J.R. Jambeck, K.L. Law, Production, use, and fate of all plastics ever made, Sci. Adv. 3 (2017), https://doi.org/10.1126/sciadv.1700782.
[2] A.L. Andrady, M.A. Neal, Applications and societal benefits of plastics, Philos. Trans. R. Soc. B 364 (2009) 1977–1984, https://doi.org/10.1098/rstb.2008.0304.
[3] Plastics Europe. Plastics – the Facts 2022. 2022.
[4] M. Shamsuyeva, H.-J. Endres, Plastics in the context of the circular economy and sustainable plastics recycling: comprehensive review on research development, standardization and market, Compos. Part C 6 (2021) 100168, https://doi.org/10.1016/j.jcomc.2021.100168.
[5] Z.O.G. Schyns, M.P. Shaver, Mechanical recycling of packaging plastics: a review, Macromol. Rapid Commun. 42 (2021), https://doi.org/10.1002/marc.202000415.
[6] K. Ragaert, L. Delva, K. Van Geem, Mechanical and chemical recycling of solid plastic waste, Waste Manag. 69 (2017) 24–58, https://doi.org/10.1016/j.wasman.2017.07.044.
[7] K. Ragaert, C. Ragot, K.M. Van Geem, S. Kersten, Y. Shiran, S. De Meester, Clarifying European terminology in plastics recycling, Curr. Opin. Green Sustain. Chem. 44 (2023) 100871, https://doi.org/10.1016/j.cogsc.2023.100871.
[8] F. Cao, L. Wang, R. Zheng, L. Guo, Y. Chen, X. Qian, Research and progress of chemical depolymerization of waste PET and high-value application of its depolymerization products, RSC Adv. 12 (2022) 31564–31576, https://doi.org/10.1039/D2RA06499E.
[9] Textile Exchange. Preferred Fiber And Materials Market Report. 2022.
[10] E. Barnard, J.J. Rubio Arias, W Thielemans, Chemolytic depolymerisation of PET: a review, Green Chem. 23 (2021) 3765–3789, https://doi.org/10.1039/d1gc00887k.
[11] Z. Fang, R.L. Smith, H. Inomata, K. Arai, Phase behavior and reaction of polyethylene terephthalate–water systems at pressures up to 173 MPa and temperatures up to 490 °C, J. Supercrit. Fluids 15 (1999) 229–243, https://doi.org/10.1016/S0896-8446(99)00010-8.
[12] M.D. Joseph, Thermal Analysis of Polymers: Fundamentals and Applications, Wiley, 2009, https://doi.org/10.1002/9780470423837.
[13] M. Pecchi, A. Cascioli, A.R. Maag, J.L. Goldfarb, M. Baratieri, Uncovering the transition between hydrothermal carbonization and liquefaction using differential scanning calorimetry, Fuel Process. Technol. 235 (2022) 107349, https://doi.org/10.1016/j.fuproc.2022.107349.
[14] M. Pecchi, F. Patuzzi, V. Benedetti, R. Di Maggio, M. Baratieri, Kinetic analysis of hydrothermal carbonization using high-pressure differential scanning calorimetry applied to biomass, Appl. Energy 265 (2020) 114810, https://doi.org/10.1016/j.apenergy.2020.114810.
[15] P. Pereira, P.E. Savage, C.W. Pester, Neutral hydrolysis of post-consumer polyethylene terephthalate waste in different phases, ACS Sustain. Chem. Eng. 11 (2023) 7203–7209, https://doi.org/10.1021/acssuschemeng.3c00946.
[16] A. Jaime-Azuara, T.H. Pedersen, R. Wimmer, Process optimization by NMR-assisted investigation of chemical pathways during depolymerization of PET in subcritical water, Green Chem. 25 (2023) 2711–2722, https://doi.org/10.1039/D2GC04831K.
[17] M. Pecchi, F. Patuzzi, V. Benedetti, R. Di Maggio, M. Baratieri, Thermodynamics of hydrothermal carbonization: assessment of the heat release profile and process enthalpy change, Fuel Process. Technol. 197 (2020) 106206, https://doi.org/10.1016/j.fuproc.2019.106206.
[18] G.P. Karayannidis, A.P. Chatziavgoustis, D.S. Achilias, Poly(ethylene terephthalate) recycling and recovery of pure terephthalic acid by alkaline hydrolysis, Adv. Polym. Technol. 21 (2002) 250–259, https://doi.org/10.1002/adv.10029.
[19] S. Ügdüler, K.M. Van Geem, R. Denolf, M. Roosen, N. Mys, K. Ragaert, et al., Towards closed-loop recycling of multilayer and coloured PET plastic waste by alkaline hydrolysis, Green Chem. 22 (2020) 5376–5394, https://doi.org/10.1039/D0GC00894J.
[20] J. Xin, Q. Zhang, J. Huang, R. Huang, Q.Z. Jaffery, D. Yan, et al., Progress in the catalytic glycolysis of polyethylene terephthalate, J. Environ. Manag. 296 (2021) 113267, https://doi.org/10.1016/j.jenvman.2021.113267.
[21] B.-K. Kim, G.-C. Hwang, S.-Y. Bae, S.-C. Yi, H Kumazawa, Depolymerization of polyethyleneterephthalate in supercritical methanol, J. Appl. Polym. Sci. 81 (2001) 2102–2108, https://doi.org/10.1002/app.1645.
[22] R. Franz, F. Welle, Contamination levels in recollected PET bottles from non-food applications and their impact on the safety of recycled PET for food contact, Molecules 25 (2020) 4998, https://doi.org/10.3390/molecules25214998.
[23] M. Rani, W.J. Shim, G.M. Han, M. Jang, Y.K. Song, S.H. Hong, Benzotriazole-type ultraviolet stabilizers and antioxidants in plastic marine debris and their new products, Sci. Total Environ. 579 (2017) 745–754, https://doi.org/10.1016/j.scitotenv.2016.11.033.
[24] C. Fleischmann, M. Lievenbrück, H. Ritter, Polymers and dyes: developments and applications, Polymers (Basel) 7 (2015) 717–746, https://doi.org/10.3390/polym7040717.
[25] Z. Pingping, M. Dezhu, Study on the double cold crystallization peaks of poly (ethylene terephthalate) (PET): 2. Samples isothermally crystallized at high

temperature, Eur. Polym. J. 35 (1999) 739–742, https://doi.org/10.1016/S0014-3057(98)00179-7.
[26] Z.-G. Wang, B.S. Hsiao, B.B. Sauer, W.G. Kampert, The nature of secondary crystallization in poly(ethylene terephthalate), Polymer (Guildf) 40 (1999) 4615–4627, https://doi.org/10.1016/S0032-3861(99)00067-1.
[27] R. Boulatov, The challenges and opportunities of contemporary polymer mechanochemistry, ChemPhysChem 18 (2017) 1419–1421, https://doi.org/10.1002/cphc.201700127.
[28] K. Pang, R. Kotek, A. Tonelli, Review of conventional and novel polymerization processes for polyesters, Prog. Polym. Sci. (Oxford) 31 (2006) 1009–1037, https://doi.org/10.1016/j.progpolymsci.2006.08.008.
[29] R. Mohan, H. Lorenz, A.S. Myerson, Solubility measurement using differential scanning calorimetry, Ind. Eng. Chem. Res. 41 (2002) 4854–4862, https://doi.org/10.1021/ie0200353.
[30] Y. Takebayashi, K. Sue, S. Yoda, Y. Hakuta, T. Furuya, Solubility of terephthalic acid in subcritical water, J. Chem. Eng. Data 57 (2012) 1810–1816, https://doi.org/10.1021/je300263z.
[31] U.W. Gedde, Essential Classical Thermodynamics, first ed., Springer, Cham, 2020 https://doi.org/10.1007/978-3-030-38285-8.
[32] M.-Y. Tang, S.L. Kim, Poly(ethyene terephthalate)-solvent interaction: gelation and melting point depression, Polym. Eng. Sci. 34 (1994) 1656–1663, https://doi.org/10.1002/pen.760342203.
[33] P. Fang, S. Xia, X. Lu, Rapid alcoholysis of PET enhanced by its swelling under high temperature, J. Environ. Chem. Eng. 10 (2022) 107823, https://doi.org/10.1016/j.jece.2022.107823.
[34] P.J. Flory, Principles of Polymer Chemistry, Cornell University Press, Ithaca, 1953.
[35] J.R. Campanelli, M.R. Kamal, D.G. Cooper, A kinetic study of the hydrolytic degradation of polyethylene terephthalate at high temperatures, J. Appl. Polym. Sci. 48 (1993) 443–451, https://doi.org/10.1002/app.1993.070480309.
[36] S. Mishra, V.S. Zope, A.S. Goje, Kinetics and thermodynamics of hydrolytic depolymerization of poly(ethylene terephthalate) at high pressure and temperature, J. Appl. Polym. Sci. 90 (2003) 3305–3309, https://doi.org/10.1002/app.13065.
[37] C.-Y. Kao, B.-Z. Wan, W.-H. Cheng, Kinetics of hydrolytic depolymerization of melt poly(ethylene terephthalate), Ind. Eng. Chem. Res. 37 (1998) 1228–1234, https://doi.org/10.1021/ie970543q.
[38] D.A.S. Ravens, I.M. Ward, Chemical reactivity of polyethylene terephthalate. Hydrolysis and esterification reactions in the solid phase, Trans. Faraday Soc. 57 (1961) 150, https://doi.org/10.1039/tf9615700150.
[39] A. Aguado, L. Martínez, L. Becerra, M. Arieta-araunabeña, S. Arnaiz, A. Asueta, et al., Chemical depolymerisation of PET complex waste: hydrolysis vs. glycolysis, J. Mater. Cycles Waste Manag. 16 (2014) 201–210, https://doi.org/10.1007/s10163-013-0177-y.
[40] N.G. Polikhronidi, I.M. Abdulagatov, G.V. Stepanov, R.G. Batyrova, Isochoric heat-capacity measurements for pure methanol in the near-critical and supercritical regions, Int. J. Thermophys. 28 (2007) 163–193, https://doi.org/10.1007/s10765-007-0164-4.
[41] N.G. Polikhronidi, I.M. Abdulagatov, G.V. Stepanov, R.G. Batyrova, Isochoric heat capacity measurements for $H_2O$ + $CH_3OH$ mixture in the near-critical and supercritical regions, Fluid Phase Equilib. 252 (2007) 33–46, https://doi.org/10.1016/j.fluid.2006.12.005.
[42] N.G. Polikhronidi, I.M. Abdulagatov, G.V. Stepanov, R.G. Batyrova, Isochoric heat capacity measurements for pure ethanol in the near-critical and supercritical regions, J. Supercrit. Fluids 43 (2007) 1–24, https://doi.org/10.1016/j.supflu.2007.05.004.
[43] NIST. 1-(Methylamino)anthraquinone n.d. https://webbook.nist.gov/cgi/cbook.cgi?ID=C82382&Mask=4 (accessed January 15, 2024).
[44] ChemSpider. Drometrizole n.d. https://www.chemspider.com/Chemical-Structure.16197.html (accessed January 15, 2024).
[45] J.N. Hahladakis, C.A. Velis, R. Weber, E. Iacovidou, P. Purnell, An overview of chemical additives present in plastics: migration, release, fate and environmental impact during their use, disposal and recycling, J. Hazard. Mater. 344 (2018) 179–199, https://doi.org/10.1016/j.jhazmat.2017.10.014.
[46] F. Wang, G. Yang, W. Zhang, W. Wu, J. Xu, Copper and manganese: two concordant partners in the catalytic oxidation of *p*-cresol to *p*-hydroxybenzaldehyde, Chem. Commun. (2003) 1172–1173, https://doi.org/10.1039/b300610g.
[47] C.V. Rode, M.V. Sonar, J.M. Nadgeri, R.V Chaudhari, Selective synthesis of *p*-hydroxybenzaldehyde by liquid-phase catalytic oxidation of *p*-cresol, Org. Process. Res. Dev. 8 (2004) 873–878, https://doi.org/10.1021/op0498619.
[48] D. Makarouni, S. Lycourghiotis, E. Kordouli, K. Bourikas, C. Kordulis, V. Dourtoglou, Transformation of limonene into *p*-cymene over acid activated natural mordenite utilizing atmospheric oxygen as a green oxidant: a novel mechanism, Appl. Catal. B 224 (2018) 740–750, https://doi.org/10.1016/j.apcatb.2017.11.006.
[49] M.A. Martín-Luengo, M. Yates, M.J. Martínez Domingo, B. Casal, M. Iglesias, M. Esteban, et al., Synthesis of *p*-cymene from limonene, a renewable feedstock, Appl. Catal. B 81 (2008) 218–224, https://doi.org/10.1016/j.apcatb.2007.12.003.